First principles calculation of configurational energy density of states for LLTO with new Wang and Landau algorithm variant

Jason D. Howard[1]

[1] *Materials Science Division, Argonne National Lab, Lemont, IL, 60439, USA*

(Dated: August 1, 2019)

In this work a variant of the Wang and Landau algorithm for calculation of the configurational energy density of states is proposed. The algorithm is referred to as B_LENDER, which is an acronym for $B_L$end Each New Density Each Round and an adjective for how it was created and functions. The algorithm was developed for the purpose of working towards the goal of using first principles simulations, such as density functional theory, to calculate the partition function of disordered sub lattices in crystal materials. The expensive calculations of first principles methods make a parellel aglorithm necessary for a practical compuation of the configurational energy density of states within a supercell approximation of a solid state material. The developed algorithm is natural to paralleize, is developed from a self consistent perspective, and was developed purposely for lattice based problems encountered in the study of disordered crystal sublattices. The algorithm develped in this work is tested with the 2d Ising model to bench mark the algorithm and to help provide insight for implementing the algorithm to a materials science application. The algorithm is then applied to the lithium and lanthanum sublattice of the solid state lihithium ion conductor $Li_{0.5}La_{0.5}TiO_3$. This was done to help understand the disordered nature of the lithium and lanthanum. The results find overall that the algorithm performs very well for the 2-d Ising model and that the results for $Li_{0.5}La_{0.5}TiO_3$ are consistent with experiment while providing additional insight into the lithium and lanthunum ordering in the material.

INTRODUCTION

For crystalline materials with disordered sub-lattices such as the Li-ion solid state electrolyte LLTO it is desirable to calculate from first principles methods(such as density functional theory[1]) the configurational energy density states $G(E_j)$. Here the energy density of states refers to the energies of the distinct lattice configurations. With the energy density of states the partition function,

$$Z = \sum_{i}^{\Omega} e^{\frac{-e_i}{k_B T}} = \sum_{j}^{\Pi} G(E_j) e^{\frac{-E_j}{k_B T}} \ , \tag{1}$$

can be determined and from it many important thermodynamics properties such as the free energy, entropy, specific heat, and ensemble averages calculated. In Eq. (1), Ω corresponds to the number of possible configurations and energies in the set $\{\Sigma_i, e_i\}_\Omega$, Π to number of possible distinct energies E_j, k_B is Boltzman's constant, and T is the temperature. One method to solve this problem could be temperature dependent simulations involving the Metropolis algorithm an sampling with probality proportional to $exp(\frac{-e_i}{k_B T})$ and histogram re-weighting techniques[2, 3]. Another more adanved method is the multi-canonical method proposed by Berg et al. [4]. A variant of multicanaonical sampling that samples the density of states directly known as entropic sampling developed by Lee [5] could also be used. These algorithms require a good estimate of the density of states to be effective. Another algorithm called the Wang and Landau algorithm [6] has been developed which is temperature independent and is based on a random walk in energy space and builds up the density of states as the algorithm progresses. An issue with these algorithms(if using a single walker) in use with first principles methods such as density functional theory is the large number of iterations needed which would require a prohibitively long wall time at the current performance power of computers. In this paper an algorithm is proposed that combines the use of random sets along with the importance sampling method of the Wang and Landau algorithm, this importance sampling is similar to the entropic sampling proposed by Lee [5]. The algorithm also used the philosophy of the Wang and Landau algorithm to build up a estimate of the density of states as the algorithm progresses. The proposed algorithm is meant to work towards the goal of a highly parallel importance sampling algorithm that directly calculates the density of states, meshes well with high performance computing architectures, and has a minimum of parmaters for implementation. The algorithm developed in this work is referred to as the B_LENDER ($B_L$end Each New Density Each Round) algorithm.

The Wang and Landau method does have parallel versions, including restricting random walkers to specific energy ranges or allowing the walkers to explore the entire space while periodically communicating with each other [7–9]. The B_LENDER algorithm is charecterized by allowing the walkers to expore the entire energy range and communication with each other through an update to the density of states at each iteration. There also have been reports of the Wang and Landau algorithm used with first principles calculations to calculate magnetic properties of materials and order to disorder properties of alloys by [10, 11]. In principle many of the different forms of the Wang and Landau sampling currently used are based

around the concept of sampling until a flat historgram of the visted energies is reached followed by a reduction in the modification factor of the density of states. There have been advancements made in understanding how to reduce the modification factor by Belardinelli et al. [12] whom developed the 1/t algorithm, this result was verified by the work of Zhou et al. [13]. The novel aspects of the B$_L$ENDER algrotihm include, a continuous adapation of the modification factor to the density of states using the current sum of the density of states as a regulator, using the number of configurations as an parameter in the modification factor, and using a histogram of the currently visited energies/configurations as a parameter in the modification factor. The algorithm in this work was also formulated in a self consistent fashion, is believed to naturally evolve to a flat histogram of the visted energy levels, and is natural to parallelize as it is based on a set of random walkers. The algorithm is not claimed to supercede or be superior to other variants of the Wang and Landau algorithm but was developed purposely for ease of use in the application to disorered sublattices of crystal systems.

In this work the formulated algorithm is benched marked with the 2d Ising model as a standard means of testing performance. The tests allow for a comparision to exact results and to previous benchmarks of other algorithms. The tests with the 2d Ising model also allow for insight in how to implement the algorithm to a materials science problem. The main goal in this work was to calculate the configurational energy density of states of the lithium ion conductor $Li_{0.5}La_{0.5}TiO_3$. This material is part of a family of possible stoiciometries $Li_{3x}La_{2/3-x}TiO_3$ of interest as solid state lithium ion conductors[14–20]. For all of the possible stoiciometries there is a tendency towards ordering of the lithium and lanthanum into lithium rich layers and lanthanum rich layers. The primary calculation of this work is that of the temperature dependant order parameter related to the lanthanum rich layer in $Li_{0.5}La_{0.5}TiO_3$. This calculation both serves to benchmark the application of the algorithm to a materials science problem with experimental knowns and to provide further insight into the physics of the material.

The rest of the article is organized as follows; section explaining and motivating the new algorithm, a section bench marking the algorithm with the 2d ising model, then a section applying the algorithm to the $Li_{0.5}La_{0.5}TiO_3$ system followed by the conclusions.

ALGORITHM

The B$_L$ENDER algorithm proposed in this work is given as follows. It is noted that the following algorithm is in terms of producing a relative density of states $G_r(E_j)^I$, where I is the iteration number.

$$
\begin{aligned}
&1.\ G_r(E_j)^I,\ \{\Sigma_s, e_s\}_{\mathcal{S}}^I \\
&2.\ \{\Sigma_s, e_s\}_{\mathcal{S}}^I \rightarrow \{\Sigma_s^{'}, e_s^{'}\}_{\mathcal{S}}^I \\
&3.\ \Sigma_s^{'I}, e_s^{'I} \rightarrow \Sigma_s^{I+1}, e_s^{I+1}\ P = \ min[1, G_r(e_s)^I / G_r(e_s^{'})^I] \\
&\ else\ \Sigma_s^I, e_s^I \rightarrow \Sigma_s^{I+1}, e_s^{I+1} \\
&4.\ G_r(E_j)^{I+1} = \\
&G_r(E_j)^I + \frac{C_o \mathcal{H}(E_j, \{e_s\}_{\mathcal{S}}^{I+1})}{[\sum_j G_r(E_j)^I]^{\frac{1}{N}}} G_r(E_j)^I = \\
&G_r(E_j)^I (1 + \frac{C_o \mathcal{H}(E_j, \{e_s\}_{\mathcal{S}}^{I+1})}{[\sum_j G_r(E_j)^I]^{\frac{1}{N}}})
\end{aligned}
\tag{2}
$$

Where $G_r(E_j)^0 \equiv [1 + \frac{C_o}{S}\mathcal{H}(E_j, \{e_s\}_{\mathcal{S}}^0)]$ with $\mathcal{H}(E_j, \{e_s\}_{\mathcal{S}})$ being a histogram function that counts the number of energies E_j in the set $\{e_s\}_{\mathcal{S}}$. In this work $\{\Sigma_s, e_s\}_{\mathcal{S}}^0$ is a randomly(uniformly) drawn set from the configuration space $\{\Sigma_i, e_i\}_\Omega$. In the second step a random change is applied to each element of the sampled set $\{\Sigma_s, e_s\}_{\mathcal{S}}^I$ to produced a "perturbed" set $\{\Sigma_s^{'}, e_s^{'}\}_{\mathcal{S}}^I$, for the Ising model this could be randomly flipping a spin. In the third step a random number is drawn between zero and one for every sampled configuration, if this number is less then the ratio of the current density of states of the unprimed to primed energies $G_r(e_s)^I / G_r(e_s^{'})^I$ then the perturbed configuration and energy $\Sigma_s^{'I}, e_s^{'I}$ goes to $\Sigma_s^{I+1}, e_s^{I+1}$, else the unperturbed configuration and energy Σ_s^I, e_s^I goes to $\Sigma_s^{I+1}, e_s^{I+1}$. This step (third) is dervied from the Wang and Landau method of sampling with probablity proportional to the inverse of the density of states. In the fourth step a histogram of the updated $\{e_s\}_{\mathcal{S}}^{I+1}$ energies is made and added (blended) into the current density of states $G_r(E_j)^I$ by multiplying by a constant C_o(which affects the convergence properties) and $G_r(E_j)^I$ divided by the sum of the density of states to the $1/N$ power. The $1/N$ power is introduced as tuning paramter to affect the convergence properties and was discovered through emprical testing with the 2-d Ising model. The fourth step is also shown in terms of multiplication which is discussed later. In this work it was found $C_o = \Omega^{\frac{1}{N}}$ was computationally efficient. After the algorithm is deemed to be complete it is necessary to re-normalize the iterated relative density of states $G_r(E_j)^f$ at the final iteration $I = f$ as follows,

$$
\begin{aligned}
&1.\ A = \sum_j G_r(E_j)^f \\
&2.\ G(E_j) \approx G_r(E_j)^f \frac{\Omega}{A}\ ,
\end{aligned}
\tag{3}
$$

to produce the properly normalized estimated value of $G(E_j)$. In principle the $G_r(E_j)$ can also be renormalized based on information of the number of configurations in

a given bin. For example if the ground state is known to have a given degenerancy then the entire density of states can be normalized such that the ground state bin has the corret degenerancy.

An important discussion point of this algorithm (Eq 2) is the update of the relative density of states(step four) being presented as addition and multiplication. In the addition form the self consistent nature of the update is clear, in the sense that the density of states is updated by adding a piece proportional to the counts in the histogram of the random set times the relative proportion of that energy level in the current estimate of the density of states. In the typical Wang and Landau sampling the update of the density of states is preformed by multiplication combined with a periodic reduction of the multiplication factor. In the multiplication form of step four of this algorithm (Eq 2) it is seen that the dependence on one over the sum of the density of states serves to naturally reduce the multiplication factor as the simulation progresses. The multiplication form is also useful when Ω is large and the sum of the density of states is larger than a typical floating point number. In this case the log of the density of states can be stored and the update performed through addition of logs. Taking $G_r^M \equiv max[G_r(E_j)]$ the log of $\sum_j G_r(E_j)^I$ can be written as,

$$G_r^{LS} \equiv \log[\sum_j G_r(E_j)^I] = \log[G_r^M \frac{\sum_j G_r(E_j)^I}{G_r^M}] = \log[G_r^M] + \log[\sum_j e^{\ln[G_r(E_j)]-\ln[G_r^M]}] \; . \tag{4}$$

With G_r^{LS} from Eq 4 the log update form of step four of the algorithm (Eq 2) can be written as the following,

$$\log[G_r(E_j)^I(1+\frac{C_o\mathcal{H}(E_j,\{e_s\}_{\mathcal{S}}^{I+1})}{[\sum_j G_r(E_j)^I]^{\frac{1}{N}}})] = \log[G_r(E_j)^I] + \log[1+\mathcal{H}(E_j,\{e_s\}_{\mathcal{S}}^{I+1})e^{\ln[C_o]-\frac{1}{N}G_r^{LS}}] \; . \tag{5}$$

In this form the alogrithm can be implemented even when Ω is large. To implement the ratio of the density of states in step two of the algorithm,

$$e^{\ln[G_r(e_s)^I]-\ln[G_r(e_s')^I]} \; , \tag{6}$$

can be used.

Analysis and generalization of algorithm

The algorithm developed in this work can be analyzed by considering the adiabatic properties of a more general historgram $\mathcal{H}(E_j,\{e_s\}_{\mathcal{S}\times\mathcal{I}})$. Where $\mathcal{H}(E_j,\{e_s\}_{\mathcal{S}\times\mathcal{I}})$ is a historgram generated with $\mathcal{S}$ walkers simulated to $\mathcal{I}$ iterations using Wang and Landau importance sampling with respect to a fixed estimate of the density of states $G_r(E_j)$. Considering that, the sampled energies are being generated with a probablility proportional to the exact density of states $G(E_j)$ and accepted with propablity inversely proportional to the relavtive(estimate) of the density of states $G_r(E_j)$, a historgram $\mathcal{H}(E_j,\{e_s\}_{\mathcal{S}\times\mathcal{I}})$ in equilibrium with $G(E_j)$ and $G_r(E_j)$ should follow the proportionality,

$$\mathcal{H}(E_j,\{e_s\}_{\mathcal{S}\times\mathcal{I}}) \propto \frac{G(E_j)/\Omega}{G_r(E_j)/A} \; . \tag{7}$$

Where A is the sum over $G_r(E_j)$. Consider here that $\mathcal{H}(E_j,\{e_s\}_{\mathcal{S}\times\mathcal{I}})$ is generated with a fixed $G_r(E_j)$ for a certain number of iterations $\mathcal{I}$, then its sum is $\mathcal{I}\times S$. So in normalizing the proportionality in Eq 7 to $\mathcal{I}\times S$ we get,

$$\mathcal{H}(E_j,\{e_s\}_{\mathcal{S}\times\mathcal{I}}) = \mathcal{S}\mathcal{I}\frac{G(E_j)}{G_r(E_j)}(\sum_j^{\Pi}\frac{G(E_j)}{G_r(E_j)})^{-1} \; . \tag{8}$$

Solving for the exact density of states gives,

$$G(E_j) = \mathcal{H}(E_j,\{e_s\}_{\mathcal{S}\times\mathcal{I}})G_r(E_j)\Phi \; , \tag{9}$$

where,

$$\Phi \equiv \sum_j^{\Pi}\frac{G(E_j)}{G_r(E_j)}\frac{1}{\mathcal{S}\mathcal{I}} \; . \tag{10}$$

A result very close to this(Eq 9) was also found by Brown et al. [21]. Another similar result, that the exact density of states is encoded in the average historgram of visited energies taken from a dynamic($G_r(E_j)$ changes) Wang and Landau simulation, was found by Zhou et al. [22]. It is important to note that Eq 9 assumes that $\mathcal{H}(E_j,\{e_s\}_{\mathcal{S}\times\mathcal{I}})$ is in equilibrium and simulated to an abritary level of precision with respect to $G(E_j)$ and $G_r(E_j)$. In general we may assume an approximately equals in Eq 9. From Eq 9 it is important to note that Φ is equivalent for all energy levels and does not affect relative probablities. In this sense we can rewrite Eq 9 as an equation for updating the relative density of states as follows,

$$G_r(E_j)^{I+1} = \mathcal{H}(E_j,\{e_s\}_{\mathcal{S}\times\mathcal{I}})G_r(E_j)^I\phi \; . \tag{11}$$

Where ϕ is now a function of our choice that is constant across energy levels at each iteration. Due to inaccuracies in $\mathcal{H}(E_j,\{e_s\}_{\mathcal{S}\times\mathcal{I}})$ and that $\mathcal{H}(E_j,\{e_s\}_{\mathcal{S}\times\mathcal{I}})$ may contain zeros Eq 11 is not a stable way to converge $G_r(E_j)$. A a better form would be "blending" some of the old and new $G_r(E_j)$ together which gives a general form of the B$_L$ENDER algorithm,

$$G_r(E_j)^{I+1} = G_r(E_j)^I + \mathcal{H}(E_j,\{e_s\}_{\mathcal{S}\times\mathcal{I}})G_r(E_j)^I\phi \; . \tag{12}$$

With Eq 12 the goal is to choose ϕ(which is a function of I) in such a way to achieve convergence. In fact the orginal form of Wang and Landau algorithm is equivalent to Eq 12 with $\mathcal{S}=1$, $\mathcal{I}=1$, and ϕ a function that decreases every time a flatness criteria of the visted energies reaches a certain threshold. For the $1/t$ algorithm $\mathcal{S}=1$, $\mathcal{I}=1$, $\log(1+\phi)$ would simply take on a m/I^p dependence. The algorithm proposed in Eq 2 is a form of this algorithm Eq 12 where the histogram is generated with Wang and Landau importance sampling with $\mathcal{I}=1$ and,

$$\phi \equiv \frac{C_o}{[\sum_j G_r(E_j)^I]^{\frac{1}{N}}} \ . \tag{13}$$

So the unique aspect of the algorithm proposed in this work is seen to be the inclusion of the histogram $\mathcal{H}(E_j,\{e_s\}_{\mathcal{S}})$ generated in parallel and the choice of ϕ in Eq 13.

An important point of discussion about Eq 12 is that for a given choice of ϕ convergence of the relative density of states is not in general guarenteed. Even for the choice in Eq 13 convergence is not necessarily guarenteed and in this work the choice is tested empirically. What can be said is that at any time the iterative process could be stopped and the histogram $\mathcal{H}(E_j,\{e_s\}_{\mathcal{S}\times\mathcal{I}})$ could be simulated to an arbitrary accuracy and then the relative density of states updated with Eq 11. In this sense Eq 12 can be determined to converge to an arbitrary accuracy if the final step is a simulation of $\mathcal{H}(E_j,\{e_s\}_{\mathcal{S}\times\mathcal{I}})$ to an abritray accuracy followed by an update with Eq 11. This is essientially the principle behind the entropic sampling form of multi-canonical simulations.

BENCH MARK WITH 2D ISING MODEL

In this work the algorithm discussed is tested using the 2d square zero field Ising model with lattice dimension of even number[23–25]. The configurations Σ_i and energies e_i of the 2d Ising model are inherently defined by the lattice site spin variables and coupling constant J. The first test is of the effectiveness of the algorithm in calculating the density of states of the 2d ising model. To test the accuracy of the simulations the results will be compared to the exact result solved by Beale [26]. The accuracy of the simulation will be determined by the error defined as,

$$\begin{aligned}\mathcal{E}(I,o) &= <|\epsilon(E_j,I,o)|>_j \\ &= \frac{1}{\Pi}\sum_{j=1}^{\Pi}\frac{|\ln(G_{ex}(E_j))-\ln(G_r(E_j,I,o))|}{|\ln(G_{ex}(E_j))|} \ .\end{aligned} \tag{14}$$

Where $G_{ex}(E_j)$ is the exact density of states, $G_r(E_j,I,o)$ is the calculated density of states at iteration number I from initial conditions and trajectory o, and $|\epsilon(E_j,I,o)|$ is the absolute value of the fractional error for a specific energy level. In Eq 14 the relative density of states $G_r(E_j,I,o)$ is renormalized according to Eq 3 prior to calculation of the error. The primed configurations in this work were generated by randomly flipping one spin on the Ising lattice

This first test of the algorithm is with the 32X32 Ising model. While the ideal value of N is not known prior to the calculation it was found in this work that a value of $N=0.1$ was computationally efficient for the 32X32 Ising model. In Fig 1 the value of the average error calculated with Eq 14 is shown up to 1e7 iterations for $S=1$, 10, 100, 1000, and $1e4$. The data in Fig 1 is averaged over 36 individual simulations for each value of S. The results show linear scaling from $S=1$ to $S=10$ and then another order of magnitude improvement from $S=10$ to $S=1000$, no significant improvement is discernable going to $S=1e4$. The periodic flucuations in the avgerage error are also noted in going to larger S, it is hypothesized that these fluctions are related to the tunneling time of the walkers. The results at $S=1000$ show that the average error is comparable to a linear speed up of the error reported for a single random walker in the orignial Wang and Landau algorithm. Defining a effective Monte Carlo step defined here as,

$$MC = \frac{S\times I}{\Pi} \ , \tag{15}$$

where Π is the number of energies. For $S=1000$, with the number of energies for the 2-d Ising model given by $n\times n$, at $I=1e7$ gives $MC\approx 1e6$. With the value of the average error being $<0.1\%$ for $S=1000$ at $MC\approx 1e6$ the B$_L$ENDER algorithm is performing very well in terms of parallel speed up as compared to the reports for the orignial Wang and Landau algorithm for a single Walker[6]. In comparison a single walker ($\mathcal{S}=1$) simulated to $MC=1e6$ using $N=0.1$ has an average error of $\approx 0.2\%$, where the result is averaged over 36 independant calculations.

In Fig 1b are also the results for average error of 36 independant simulations for 10×10 Ising model for the different number walkers $\mathcal{S}$ with $N=1$. The results show that the scaling is quite good as the number of walkers increases. This result is encouraging becuase the number of configurations that will be typical for a supercell approximation in a first principles calculation is not expected to exceed the large number of $\approx 10^{30}$ configurations in the 10×10 Ising model. This test on the smaller model indicates the algorithm is suitable for implementation in the materials science problem tackled in this paper.

Another aspect of the algorithm to consider is the dependence on the value of N and of C_o. In Fig 2 the dependence on N is shown for the 32X32 and 10X10 Ising models, simulated to $I=1e7$ and $I=1e6$ respectively,

(a)

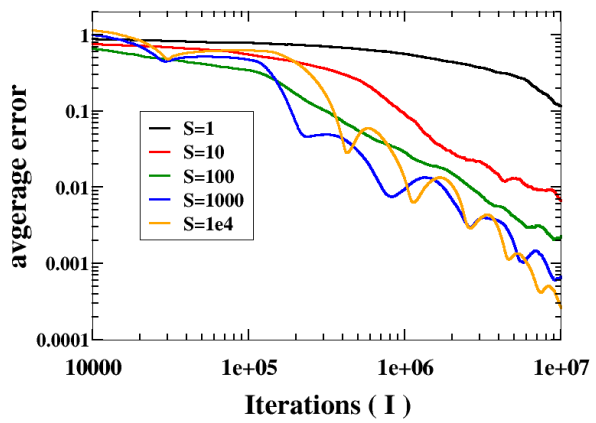

(b)

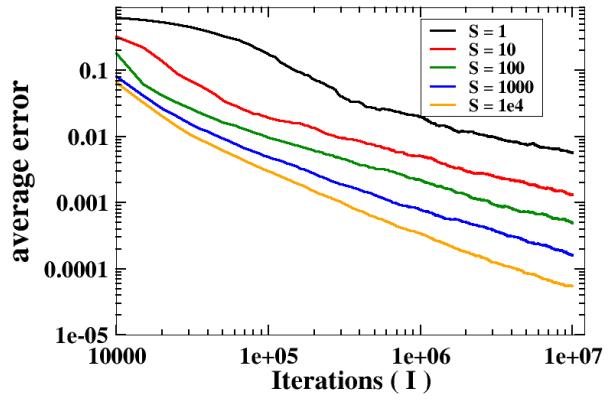

FIG. 1. Average error from 36 simulations calculated from Eq 14 with $\mathcal{S} = 1$, 10, 100, 1000, and 1e4 for (a) the 32×32 Ising model with $1/N = 0.1$, (b) the 10×10 Ising model with $1/N = 1$.

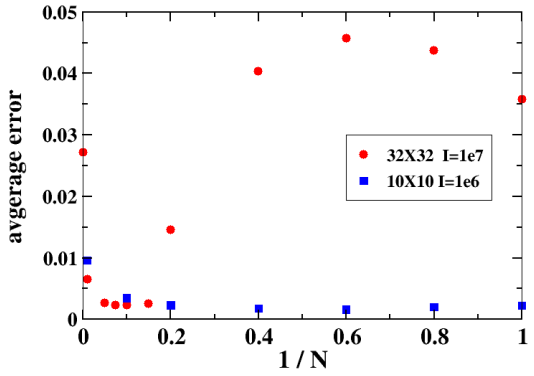

FIG. 2. Average error from 36 simulations calculated from Eq 14 vs the value of $1/N$ for the 32×32 Ising model simulated to 1e7 iterations as red circles and the 10×10 Ising model simulated to 1e6 iterations as blue squares.

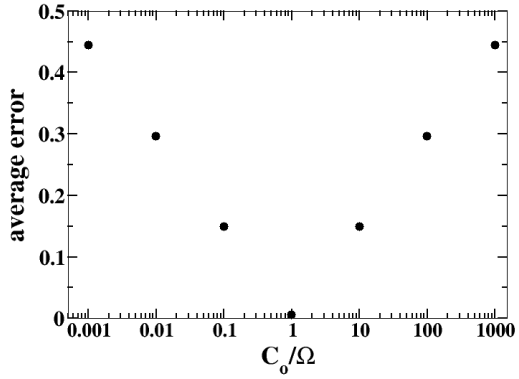

FIG. 3. Average error from 36 simulations calculated from Eq 14 for the 10×10 Ising model with $1/N = 1$ vs the value of C_o.

with $\mathcal{S} = 100$, and averaged over 36 independant calculations. The results show that for the larger 32X32 model the dependence on N is more pronounced and that the optimal value of N is lower than for the smaller 10X10 model. Previous tests have used a value of $C_o = \Omega^{1/N}$, this value was based on tests showing this to be an optimal value. In Fig 3 is shown the error for a 10×10 Ising model vs $C_o/\Omega^{1/N}$ with $N = 1$ simulated to 1e7 iterations averaged over 36 independant runs. The results in Fig 3 show that the optimal value of C_o is at $\Omega^{1/N}$.

The final part of this section is a compuatational test of Eq 8. To do this, first a 10×10 Ising model was simulated to 2.7% error to generate a $G_r(E_j)$. Then a set of 10 walkers was simulated to 1e9 iterations with Wang and Landau importance sampling with respect to this fixed $G_r(E_j)$. In Fig 4 are shown plots of the ratio of the exact density of states $G(E_j)$ to the approximate relative density of states $G_r(E_j)$ and

$$H(E_j) \equiv \mathcal{H}(E_j, \{e_s\}_{\mathcal{S}\times\mathcal{I}}) \frac{(\sum_j^{\Pi} \frac{G(E_j)}{G_r(E_j)})}{\mathcal{S}\mathcal{I}} \,. \qquad (16)$$

The agreement between theory and experimet(numerical) is seen to be exact within the visible precision of the plot, there as providing evidence for the valididity of Eq 8.

APPLICATION TO LLTO

The purpose of developing the B$_L$ENDER algorithm was to develop and algorithm suitable for the needs of solid state density functional theory calculations of disordered lattice materials. Due to the long run time of density functional theory calculations the parallel nature

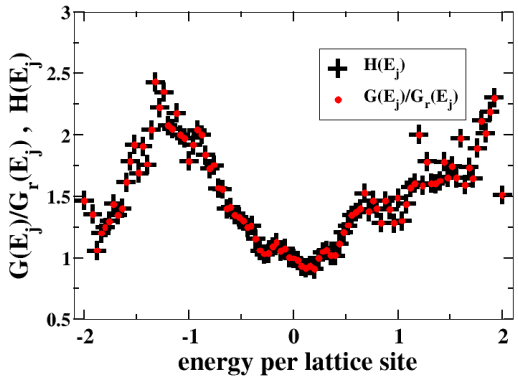

FIG. 4. Red circles show the ratio of the exact density of states $G(E_j)$ to a estimate of the relative density of states $G_r(E_j)$ for the 10×10 Ising model. This is compared to a prediction shown as black crosses made through Eq 16 calculated from a histogram of the visited energies from a simulation with fixed $G_r(E_j)$ using Wang and Landau importance sampling simulated to 1e9 iterations.

of B$_L$ENDER allows for calculations of each energy to be done as independant job submissions to a computer cluster. The results can then be processed by a script running on the head node. In this work the B$_L$ENDER algorithm is applied to the lithium and lanthanum sub lattice of the solid state lithium ion electrolyte $Li_{0.5}La_{0.5}TiO_3$. The goal of this study was to both, perform a calculation with B$_L$ENDER of a real material system that is fairly well understood, and also to learn something new in the process. Specifically the desired knowledge to be gained is a better understanding the disordering of the lithium and lanthanum sub lattice and associated lattice distoritions.

Background on LLTO

LLTO is a complex material comprised of a variety of stoiciometries and phases but in this work the study is restricted to the reported tetragonal P4mmm phase of the stoiciometry $Li_{0.5}La_{0.5}TiO_3$[15, 19]. A unit cell of this structure is shown in Fig 5. The lattice parameters for this unit cell were taken from the experimental results from Ibarra et al.[15]; 3.8688(4)$\AA$ for a and b axes, and 7.7463(2) for c-axis. This unit cell is representative of an ordered form of $Li_{0.5}La_{0.5}TiO_3$ where the lithium and lanthunum are seperated into seperate layers on the high symettry A-sites. Where the A-site refers to the general pervoskite formula unit ABX_3. The structure in Fig 5 is actually strucutrally unstable and the energy can be lowered by lattice disortions which manifests as tilts in the titaninum oxygen octehedra and the lithium and lanthum distoriting off of the high symettry A-sites. The instablity of the structure in Fig 5 is evidenced by the imaginary phonon modes calculated by Moriwake et al. [16].

The physics of interest in this study is to understand the disordering of lithium and lanthanum between layers. It is reported for this phase that the lanthanum are mostly mixed between layers when the samples are slow cooled during synthesis and if quenched from high temperature the lanthanum ordering is reported to be completely mixed between layers [15]. Apart from the mixing of lithium and lanthum between layers there is also configurational complexity associated with octahedral tilting. In this work the B$_L$ENDER algorithm is used to evaluate the density of configuration states associated with local minium corresponding to both the litihium and lanthanum ordering and lattice distortions.

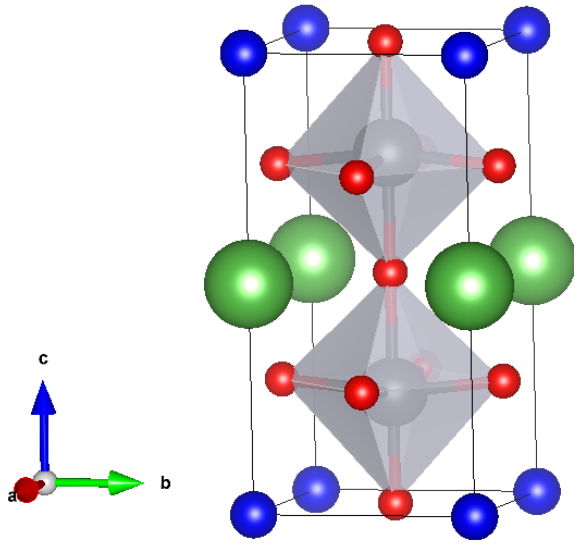

FIG. 5. 10 atom unit cell of P4/mmm $Li_{0.5}La_{0.5}TiO_3$. Where dark blue balls are lithium, green balls are lanthanum, red balls are oxygen, and grey balls inside of octahedra are titaniu.

Computational Details

In this work a 3×3×1 supercell of the unit cell shown in Fig 5 was used as an approximation bulk $Li_{0.5}La_{0.5}TiO_3$. While not an ideal size as it is still restrictive of the possible lattice configurations and to the types of domains of octehedral tilting that can form it is the largest supercell practical for performing the configurational Monte-Carlo in this work.

An important aspect of completing this study is a scheme for producing the initial and primed configurations in the iterative process of the B$_L$ENDER algorithm. The scheme used in this study was to first generate a

set of lithium and lanthanum randomly placed on the high symettry A-sites where occupancy is restricted to one, then a small amount of noise on the order of $\pm 0.2\mathring{A}$ was added to each lithium and lanthanum cooridnate. These configurations were then relaxed to a local minimum which formed the first set of configurations in the iterative process. Then the primed configurations (step 2) were formed by swapping a random lithium and lanthum atom and placing them back on the high symmetry A-site along with a new amount of random noise, these configurations where then relaxed to a local minimum. The random noise off the A-site served to allow for searching the distorted lattice configuration space.

The methods used in the calculation of the total energies of the lattice configurations of LLTO in this work was density functional theory using the VASP code. The PBE variant of generalized gradient approximation was used for the exchange and correlation functional. Wave functions were represented by a plane wave basis with a 250eV cut off and self consistent cycles were converged with a energy difference of 2.5e-5 eV. The k-point mesh was 1X1X2 gamma centered for the 3X3X1 supercells of the LiTiO6 unit cell. The calculations were performed at the experimental lattice paramaters $3.8688\mathring{A}$ for a and b axes, and 7.7463 for c-axis. The paramaters for the B_LENDER algorithm were $\mathcal{S} = 10$ and $N = 1$. The bin width used for determining $G_r(E_j)$ was choosen to 0.02eV. This value in bin width is approximately the same as relative errors in the calculations arising from the numerical details of the specified convergence paramaters. The value of omega was estimated as 10 times the combinatoric number of configurations of the lithium and lanthanum ordering onto the A-site given as,

$$\Omega \approx 10\frac{18!}{9!9!} \, . \tag{17}$$

While an exact value of Ω is not needed for the algorithm to converge experience suggests that being close as possible is computationally beneficial. Estimating that Ω is greater than the combinatoric calculation of the lithium and lanthanum in the A-site cages comes from the possibility of multiple distinct lattice distoritions for each type of A-site cage configuration.

Results

Using the paramters and configurational enumeration scheme specified above a simulation was performed to 800 iterations for the 3×3×1, 90 atom supercell. After 150 iterations the algorithm was restricted to look in the energy range less than 1.25eV higher than the lowest energy found at that time. This was to improve compuatational efficiency by preventing the walkers from exploring an unnecessarily high energy range. While 800 iterations is likely not ideally converged, some indication of convergence can be understood by comparing the results at 400 iterations to those at 800 iterations. It is expected that the qualititave aspects of the results are well accounted for despite the limited number of iterations.

The main focus of the results is the nature of the lithium and lanthanum sublattice ordering. To accomplish this the order parameter of interest is that of the occupancy of lanthanum in the lanthanum rich layer along the c-axis. In the work by Ibarra et al. [15] they refer to this order paramater as $La1^c$, the same convention will be used in this work. In this work the order parameter of the lanthanum rich layer along the equivalent a and b axes denoted as $La1^{a,b}$ is also studied. This is of interest becuase the system is neary cubic it is expected that the layering along the a and b axis should have similar energetics to that along the c-axis. These two order paramters, $La1^c$ and $La1^{a,b}$, are defined as the number of lanthanum in the lanthanum rich layer divided by the total number that could occupy the layer. As an example the unit cell in Fig 5 woud have $La1^c = 1$ and $La1^{a,b} = 0.5$ It is important to note in this work the 3×3×1 supercell restricts the configurations along the a and b axis from having altenerate layering of lithium and lanthanum rich layers. Ideally the calculations would be done with at least a 4×4×1 supercell but the computational effort is beyond the scope of this work. The results later will have to be interpreted taking this systematic supercell error into account.

To calculate the ensemble average of these order paramaters first arithmetic averages of the order parameter at each energy level E_j are calculated from the primed configurations ($\{\Sigma_s^{'}\}$) that occurred during the simulation. The arithmetic average of a general order parameter O over all configurations with energy E_j is denoted by $< O >_j$. Then with these the ensemble average is computed as,

$$\langle O \rangle = \sum_{j=1}^{\Pi} < O >_j \, G_r(E_j) \frac{e^{-\frac{E_j}{k_B T}}}{Z} \, . \tag{18}$$

Where $Z = \sum_{j=1}^{\Pi} G_r(E_j) exp(-\frac{E_j}{k_B T})$. It is noted that normalization of the relative density of states to the appropriate number of configurations is not necessary for the calculation of the ensemble average of an order parameter. If wanting to compare free energies($-k_B T \ln(Z)$) between phases it would be necessary to normalize the density of states properly to obtain an accurate calculation of the free energy.

The first main result to report is a view of the convergence of $G_r(E_j)$ as a function of the iterations. In Fig 6 $G_r(E_j)$ is shown at $I =$, 150, 300, and 600 with the y-axis plotted on a log scale. The $G_r(E_j)$ shown in Fig 6 are plotted such that the lowest energy of $G_r(E_j)$ found at the particular iteration show is set to zero, the sharp

(a) 150 iterations

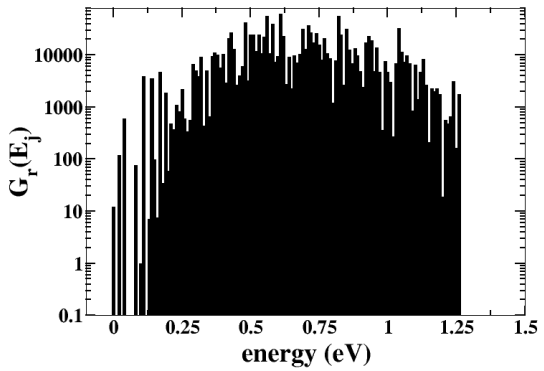

(b) 300 iterations

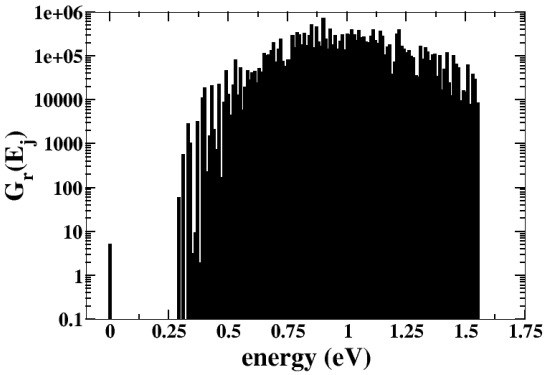

(c) 600 iterations

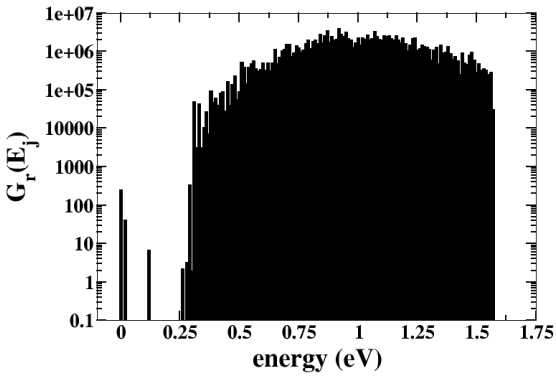

FIG. 6. Plots of $G_r(E_j)$ at (a) 150 iterations, (b) 300 iterations, and (c) 600 iterations. The plots are normalized by dividing through by the smallest value of $G_r(E_j)$ at that particular iteration. The plots are shown with a log scale on the y-axis.

cutoff at higher energy was the upper limit to configurational search, and the plots are normalized by dividing through by the minimum of $G_r(E_j)$ at that iteration. The main characteristic of the results by 600 iterations is the presence of some low energy states with a energy gap up to a more continous spectrum of states. These low energy states (<0.25 eV) at 600 iterations are characterized as have $La1^c = 1$, that being having alternate layers of lithium and lanthanum along the c-axis. They are not however equivelent to the unit cell shown in Fig 5, in that the structures have distinct lattice disortions.

(a)

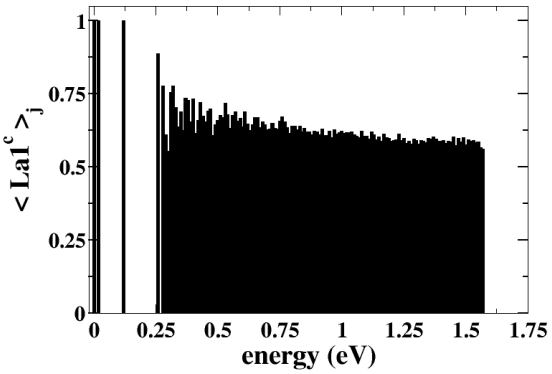

(b)

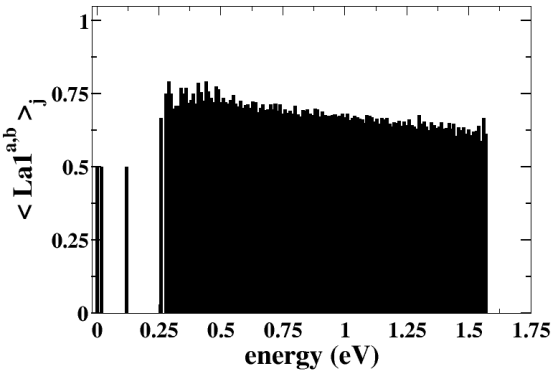

FIG. 7. Plots of the arithmetic averages of $La1^c$ (a) and $La1^{a,b}$ (b) at each energy level sampled during the Monte-Carlo simulation.

The next result is the arthimetic averages of the $La1^c$ and $La1^{a,b}$ order parameters. These are shown in Fig 7. The results show that expect for the lowests energies there is a tendency at the lower energies for layering of the lanthanum along all axis. The lowest energies come from layering along the alternate lanthanum lithium layering along the c-axis. At higher energies the results show a tendency of a decrease in the amount of lanthanum in the lanthanum rich layer along all axes. This is consistent with the notion of the material being more disordered at higher energies. With these results the ensemble averages can are computed with Eq 18, these results are shown in Fig 8. The results show the characteristics of an order to disorder transition where the system goes from being

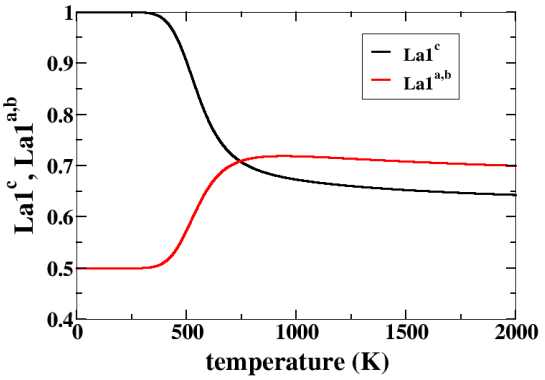

FIG. 8. Ensemble average order parameters as function of temperature for $La1^{c}$ in black and $La1^{a,b}$ in black.

completely layered along the c-axis to the system being disordered. This transition is predicted to initiate at approximately 400K. This transition is also evidenced in a spike in the heat capacity shown in Fig 9, calculated from the derivate with respect to temperature of the ensemble average of the total energy of the system. Although in the disordered region of Fig 8 the value of the order parameters indicates there is both a preference for lanthanum rich layers along all axis. It is likely that this preference for lanthanum rich layers along any axis would result in complex domain formation within the bulk material. In fact other stoichiometries are know to exhibit domain formation related to the ordering of lanthanum rich layers.

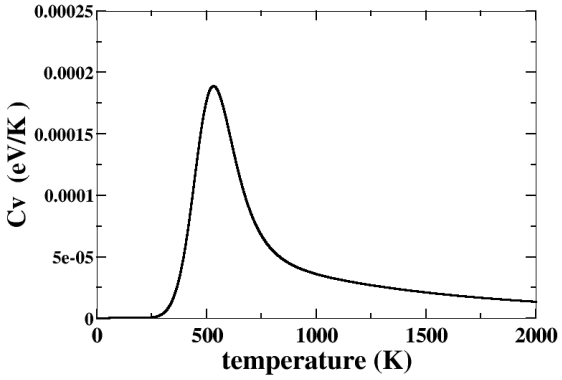

FIG. 9. Heat capacity per $LiLaTi_2O_6$ unit cell.

With the analytic results of the ensemble averaged order parameters and the heat capacity much has been learned about the overall all ordering tendancy of the lanthanums. Although it is not feasible to show visually all of the various strucutures found during the Monte-Carlo search some of the lower energy strucutures will be shown to give further insight.

This work was supported by the Center for Electrical Energy Storage: Tailored Interfaces, an Energy Frontier Research Center funded by the US Department of Energy, Office of Science, Office of Basic Energy Sciences at Argonne National Laboratory under Contract DE-AC02-06CH11357. I would like to thank the Laboratory Computing Resource Center (LCRC) faculty of Argonne National Lab for their support and maintenance of the computing resources that made this project possible.

[1] W. Kohn and L. J. Sham. Self-consistent equations including exchange and correlation effects. *Phys. Rev.*, 140:A1133–A1138, 1965.

[2] N. Metropolis, A. W. Rosenbluth, M. N. Rosenbluth, A. H. Teller, and E. Teller. Equation of state calculations by fast computing machines. *J. Chem. Phys.*, 21(6):1087–1092, 1953.

[3] D. P. Landau and K. Binder. *A Guide to Monte Carlo Simulations in Physics*. Cambridge University Press, fourth edition edition, 2015.

[4] Bernd A. Berg and Thomas Neuhaus. Multicanonical ensemble: A new approach to simulate first-order phase transitions. *Phys. Rev. Lett.*, 68:9–12, Jan 1992.

[5] Jooyoung Lee. New monte carlo algorithm: Entropic sampling. *Phys. Rev. Lett.*, 71:211–214, Jul 1993.

[6] F. Wang and D. P. Landau. Efficient, multiple-range random walk algorithm to calculate the density of states. *Phys. Rev. Lett.*, 86:2050–2053, Mar 2001.

[7] J. Yin and D. P. Landau. Massively parallel wanglandau sampling on multiple gpus. *Comput. Phys. Commun.*, 183(8):1568 – 1573, 2012.

[8] L. Zhan. A parallel implementation of the wanglandau algorithm. *Comput. Phys. Commun.*, 179(5):339 – 344, 2008.

[9] T. Vogel, Y. W. Li, T. Wüst, and D. Landau. Generic, hierarchical framework for massively parallel wang-landau sampling. 110:210603, 05 2013.

[10] M. Eisenbach, D. M. Nicholson, A. Rusanu, and G. Brown. First principles calculation of finite temperature magnetism in fe and fe3c. *Journal of Applied Physics*, 109(7):07E138, 2011.

[11] S. N. Khan and Markus Eisenbach. Density-functional monte-carlo simulation of cuzn order-disorder transition. *Phys. Rev. B*, 93:024203, Jan 2016.

[12] R. E. Belardinelli and V. D. Pereyra. Wang-landau algorithm: A theoretical analysis of the saturation of the error. *The Journal of Chemical Physics*, 127(18):184105, 2007.

[13] Chenggang Zhou and Jia Su. Optimal modification factor and convergence of the wang-landau algorithm. *Phys. Rev. E*, 78:046705, Oct 2008.

[14] Xiang Gao, Craig A. J. Fisher, Teiichi Kimura, Yumi H. Ikuhara, Akihide Kuwabara, Hiroki Moriwake, Hideki Oki, Takeshi Tojigamori, Keiichi Kohama, and Yuichi Ikuhara. Domain boundary structures in lanthanum lithium titanates. *J. Mater. Chem. A*, 2:843–852, 2014.

[15] J Ibarra, A Vrez, C Len, J Santamara, L.M Torres-Martnez, and J Sanz. Influence of composition on

the structure and conductivity of the fast ionic conductors la2/3xli3xtio3 (0.03x0.167). *Solid State Ionics*, 134(3):219 – 228, 2000.

[16] Hiroki Moriwake, Xiang Gao, Akihide Kuwabara, Craig A.J. Fisher, Teiichi Kimura, Yumi H. Ikuhara, Keiichi Kohama, Takeshi Tojigamori, and Yuichi Ikuhara. Domain boundaries and their influence on li migration in solid-state electrolyte (la,li)tio3. *Journal of Power Sources*, 276:203 – 207, 2015.

[17] H.X. Geng, A. Mei, C. Dong, Y.H. Lin, and C.W. Nan. Investigation of structure and electrical properties of li0.5la0.5tio3 ceramics via microwave sintering. *Journal of Alloys and Compounds*, 481(1):555 – 558, 2009.

[18] Anatolii Belous, Oleg Yanchevskiy, Oleg V'yunov, Odile Bohnke, Claude Bohnke, Franoise Le Berre, and Jean-Louis Fourquet. Peculiarities of li0.5la0.5tio3 formation during the synthesis by solid-state reaction or precipitation from solutions. *Chemistry of Materials*, 16(3):407–417, 2004.

[19] S. Stramare, V. Thangadurai, and W. Weppner. Lithium lanthanum titanates: a review. *Chemistry of Materials*, 15(21):3974–3990, 2003.

[20] Michele Catti. First-principles modeling of lithium ordering in the llto (lixla2/3-x/3tio3) superionic conductor. *Chemistry of Materials*, 19(16):3963–3972, 2007.

[21] G. Brown, Kh. Odbadrakh, D. M. Nicholson, and M. Eisenbach. Convergence for the wang-landau density of states. *Phys. Rev. E*, 84:065702, Dec 2011.

[22] Chenggang Zhou and R. N. Bhatt. Understanding and improving the wang-landau algorithm. *Phys. Rev. E*, 72:025701, Aug 2005.

[23] R. J. Baxter. *Exactly Solved Models in Statistical Mechanics*. Elsevier, 2016. ISBN 978-0-12-083180-7.

[24] L. Onsager. Crystal statistics. i. a two-dimensional model with an order-disorder transition. *Phys. Rev.*, 65:117–149, 1944.

[25] B. M. McCoy and T. T. Wu. *The Two-Dimensional Ising Model*. Harvard University Press, 1973.

[26] P. D. Beale. Exact distribution of energies in the two-dimensional ising model. *Phys. Rev. Lett.*, 76:78–81, Jan 1996.